Transmission Zeeman beat spectroscopy: Application to the $4f^6 6s^2\,{}^7F$ ground-level term of Sm I

R. J. McLean, P. Hannaford, and R. M. Lowe
Commonwealth Scientific and Industrial Research Organization, Division of Materials Science and Technology, Clayton, Victoria 3168, Australia
(Received 15 May 1990)

A spectroscopic technique for the accurate determination of multipole relaxation rates in ground- or near-ground atomic levels is described. The technique is based on the detection of Zeeman quantum beats in transmission geometry and yields relaxation rates for the destruction of both orientation and alignment. Collisional depolarization cross sections are reported for the $4f^6 6s^2\,{}^7F_J$ ($J=1-6$) ground-term levels in samarium I by various rare-gas perturbers. For the ${}^7F_1$ level the ratios of the cross sections for the destruction of orientation and alignment are unusually large ($\sigma_1/\sigma_2 \approx 1.6$ for each of the rare-gas perturbers), whereas for the $J=2-6$ levels the reverse is true (σ_1/σ_2 in the range 0.39 to 0.46 for argon perturbers). These values of σ_1/σ_2 are found to be in agreement with the predictions of a weak-collision model in which the collision interaction has an essentially pure quadrupole character. The observed cross sections for the ${}^7F_1$ level appear to be the first experimental realization of the simple theoretical result, $\sigma_1/\sigma_2=\frac{5}{7}$, initially obtained by Omont [J. Phys. (Paris) **26**, 26 (1965)].

I. INTRODUCTION

Quantum beats, resulting from the time evolution of a coherent superposition of nondegenerate atomic states, are most commonly detected in spontaneously emitted fluorescence from excited levels.[1] However, they may also be detected by other techniques, such as monitoring changes in the transmission of a probe beam in a pump-probe experiment with the sample between crossed or nearly crossed polarizers, as in polarization spectroscopy.[2] This *transmission* quantum beat method, first demonstrated by Lange and Mlynek,[3] is sensitive to pump-laser-induced coherences not only in the upper level but also in the lower level of a transition and has thus permitted the observation of quantum beats in ground or near-ground levels of atomic systems such as Na I,[4-7] Tl I,[8] and Sm I.[4,9]

In a previous paper[9] we presented a preliminary account of a technique based on transmission quantum beat spectroscopy for the determination of relaxation rates of both orientation and alignment in ground or near-ground atomic levels. Depolarization rates in such levels cannot be determined by conventional methods that involve detection of fluorescence from excited levels. In this transmission Zeeman beat technique a short, broadband pulse of resonant laser radiation generates coherence between nondegenerate Zeeman states of a low-lying atomic level by absorption and stimulated (or spontaneous) emission processes, and, with an appropriate choice of experimental geometry, the evolution of either orientation ($k=1$) or alignment ($k=2$) coherences in the level is monitored by recording the time dependence of the transmission of a weak cw probe laser through nearly crossed polarizers. In this paper we describe the theoretical basis of the method and demonstrate its application to the determination of collisional relaxation rates of orientation and alignment in the $J=1-6$ levels of the $4f^6 6s^2\,{}^7F$ ground-level term of Sm I. Knowledge of multipole relaxation rates in these levels has been important for the interpretation of a number of recently reported nonlinear laser experiments, including the nonlinear Hanle effect,[10] collision-induced Hanle resonances in four-wave mixing,[11] nonlinear magneto-optical rotation,[12-15] and polarization switching in an optical cavity.[16] A related polarization-rotation transient technique for measuring multipole relaxation rates in *excited* levels, but not involving quantum beats, has previously been reported by Ghosh *et al.*[17]

The present paper has the following form. In Sec. II we describe the theoretical basis of the transmission Zeeman beat technique. In Sec. III the experimental details are outlined, and the results are presented in Sec. IV. The measured collisional depolarization cross sections are discussed and compared with some simple theoretical results in Sec. V.

II. THEORY

The experimental geometry is defined in Fig. 1. The pump and probe beams counterpropagate along the Oz axis through an optically thin atomic vapor which is subjected to a small transverse magnetic field $\mathbf{B}$ in the x direction. The probe beam is weak, linearly polarized, and has a frequency ω tuned close to the transition frequency ω_0 between the lower level l and an upper level u. In the absence of background birefringence and polarizer imperfections, the intensity of the probe transmitted through the polarizers that are at angle θ from being exactly crossed is given by (see, for example, Ref. 18)

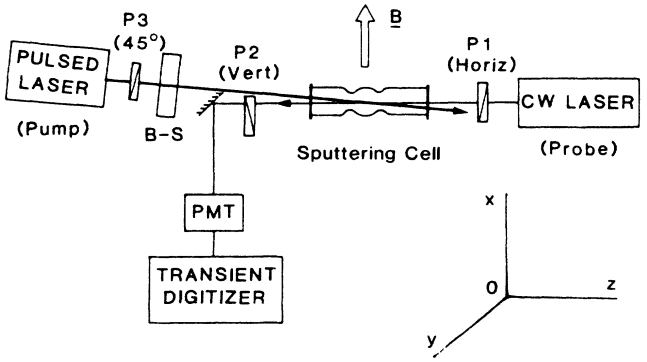

FIG. 1. Schematic diagram of experimental arrangement: P1, P2, and P3 polarizers; BS, Babinet-Soleil compensator; PMT, photomultiplier tube.

$$I \propto \theta^2 - \frac{\theta\omega L}{c}\mathrm{Re}(n^+ - n^-) + \left[\frac{\omega L}{2c}\mathrm{Re}(n^+ - n^-)\right]^2 + \left[\frac{\omega L}{2c}\mathrm{Im}(n^+ - n^-)\right]^2 , \quad (1)$$

where n^+ and n^- are the complex refractive indices of the atomic medium for the right and left circular components of the linearly polarized probe beam, and L is the length of the atomic sample. The term θ^2 accounts simply for the steady-state transmission through the nearly crossed polarizers, while in the present work the other terms are related to the anisotropy of the atomic medium due to the lower-level Zeeman coherence induced by the pump laser pulse. The quantity $\mathrm{Re}(n^+ - n^-)$ represents circular birefringence resulting from a change in the relative phase of the two circular components which leads to a rotation of the plane of polarization of the beam, while $\mathrm{Im}(n^+ - n^-)$ corresponds to circular dichroism resulting from a difference in the absorption of the two components which causes the polarization to become elliptical.

The interaction of the atomic system with the probe field may be described using atomic density-matrix equations (for example, Ref. 19) in which the probe electric field is represented classically by

$$\mathbf{E}(t) = E_0\hat{\epsilon}e^{-i\omega t} + E_0\hat{\epsilon}^* e^{i\omega t} , \quad (2)$$

where $\hat{\epsilon}$ is a unit vector in the direction of polarization of the probe electric field. E_0 is taken to be real. In this section we develop the theory for a $J_l = 1$ to $J_u = 0$ atomic transition, the simplest probe transition with which we have used the technique. The quantization axis is taken to be along Ox, i.e., parallel to $\mathbf{B}$. It is a straightforward matter to write down the equations of motion of the optical coherence components for a single velocity group of atoms, using irreducible components of the density matrix, and assuming the probe beam is polarized at an angle β to $\mathbf{B}$, i.e., $\hat{\epsilon} = \mathbf{e}_x\cos\beta + \mathbf{e}_y\sin\beta$:

$$\frac{\partial}{\partial t}\rho_0^1(lu) = -[\Gamma_1(lu) + i\delta]\rho_0^1(lu) - \frac{\Omega}{2}\sin\beta[\mathrm{Re}\rho_1^1(l) + i\,\mathrm{Im}\rho_1^2(l)] + \frac{i\Omega}{2}\cos\beta[\tfrac{4}{3}\rho_0^0(u) - \tfrac{1}{3} + \sqrt{2/3}\rho_0^2(l)] , \quad (3a)$$

$$\frac{\partial}{\partial t}\rho_1^1(lu) = -[\Gamma_1(lu) + i(\delta + \omega_L)]\rho_1^1(lu) - \frac{\Omega}{2\sqrt{2}}\sin\beta\left[\frac{4}{3}\rho_0^0(u) - \frac{1}{3} - \frac{1}{\sqrt{2}}\rho_0^1(l) - \frac{1}{\sqrt{6}}\rho_0^2(l) - \rho_2^2(l)\right] + \frac{i\Omega}{2\sqrt{2}}\cos\beta[\rho_1^1(l) + \rho_1^2(l)] , \quad (3b)$$

$$\frac{\partial}{\partial t}\rho_{-1}^1(lu) = -[\Gamma_1(lu) + i(\delta - \omega_L)]\rho_{-1}^1(lu) - \frac{\Omega}{2\sqrt{2}}\sin\beta\left[\frac{4}{3}\rho_0^0(u) - \frac{1}{3} + \frac{1}{\sqrt{2}}\rho_0^1(l) - \frac{1}{\sqrt{6}}\rho_0^2(l) - \rho_2^2(l)\right] + \frac{i\Omega}{2\sqrt{2}}\cos\beta[\rho_{-1}^1(l) - \rho_{-1}^2(l)] . \quad (3c)$$

$\delta = \omega - \omega_0$ is the laser-atom detuning of the atomic velocity group. Only the components of the optical coherences with optical frequencies are retained (for example, Ref. 19). The rate at which the optical coherences relax, $\Gamma_1(lu)$, includes a collisional component as well as radiative decay. The quantity ω_L is the Larmor precession frequency and $\Omega = (2/\sqrt{3})d_{ul}E_0$ is the Rabi frequency, where d_{ul} is the reduced dipole matrix element. We have assumed the total population for the velocity group is unity, i.e., $\rho_0^0(u) + 3^{1/2}\rho_0^0(l) = 1$, and that there is no coupling between different velocity groups, i.e., velocity-changing collisions are neglected in these equations.

The probe beam is assumed to be weak enough that the components of alignment and orientation that it induces in the lower level are negligible compared with those induced by the pump-laser pulse. In the interpretation of the present experiments the components of orientation and alignment appearing in Eqs. (3) are therefore considered to be those induced by the pump laser. Such components induced by the short pump pulse at time $t = 0$ subsequently evolve in the magnetic field according to

$$\rho_q^k(l)_t = \rho_q^k(l)_{t=0}\exp[-(\Gamma_k(l) + iq\omega_L)]t . \quad (4)$$

The relaxation rate for the 2^k multipole in the lower level, $\Gamma_k(l)$, has no radiative component, and may be expressed in the usual way as

$$\Gamma_k(l)=N\bar{v}\sigma_k ,$$

where N is the number density of rare-gas perturber atoms, $\bar{v}$ the mean relative velocity between the sample atoms and the rare-gas atoms, and σ_k the velocity-averaged collision cross section for the destruction of the multipole. In general, σ_k is the sum of two contributions:

$$\sigma_k=\Lambda_k+\sigma_0 , \tag{5}$$

where Λ_k accounts for collisions that mix the Zeeman states within the level and σ_0 accounts for collisions that depopulate the level.

The probe electric field given by Eq. (2) induces the macroscopic dipole moment

$$\mathbf{P}(t)=\mathbf{P}_0 e^{-i\omega t}+\text{c.c.}$$

in the atomic sample. The amplitude $\mathbf{P}_0=\chi\epsilon_0 E_0\hat{\epsilon}$ has components $\mathbf{P}_0^{\pm}$ with complex electric susceptibilities χ^+ and χ^- corresponding to the right and left circular components of the probe field. The components $\mathbf{P}_0^{\pm}$ may also be expressed as $\mathbf{P}_0^{\pm}=N\langle\mathbf{d}\rangle^{\pm}$, where $\langle\mathbf{d}\rangle^{\pm}$ are the components of the expectation value of the electric dipole moment induced in a single atom by the circular components of the probe field, and $\langle\mathbf{d}\rangle=\mathrm{Tr}(\rho\mathbf{d})$. The components of the unit polarization vectors defined by $\mathbf{e}_{\pm}=\mp 2^{-1/2}(\mathbf{e}_x\pm i\mathbf{e}_y)$ are $e_{\pm}=\mp 2^{-1/2}(\cos\beta\pm i\sin\beta)$ for the right and left circular components of the linearly polarized probe field.

Evaluating the trace yields

$$(\chi^+-\chi^-)\propto\cos\beta[\hat{\rho}_1^1(lu)+\hat{\rho}_{-1}^1(lu)] +i\sin\beta[\hat{\rho}_1^1(lu)-\hat{\rho}_{-1}^1(lu)] ,$$

where, for convenience, the quantization axis has been assumed to be along the direction of propagation of the probe beam Oz [indicated by the notation $\hat{\rho}_1^1(lu)$]. Following a rotation transformation of the density-matrix elements, the corresponding expression for $(\chi^+-\chi^-)$ for quantization along the magnetic-field direction is found:

$$(\chi^+-\chi^-)\propto\cos\beta[\rho_1^1(lu)+\rho_{-1}^1(lu)] -2^{1/2}i\sin\beta\rho_0^1(lu) . \tag{6}$$

Since $n\approx 1$, $n^{\pm}\approx 1+\frac{1}{2}\chi^{\pm}$ and this expression gives the induced circular birefringence and dichroism. In particular, if the polarization of the probe beam is chosen to be in the y direction, perpendicular to the magnetic field ($\beta=\pi/2$), then we have from Eqs. (6) and (3a) that

$$(n^+-n^-)\propto i\rho_0^1(lu)\propto-\frac{\mathrm{Im}\rho_1^2(l)+i\,\mathrm{Re}\rho_1^1(l)}{\Gamma_1(lu)+i\delta} . \tag{7}$$

This solution does not include transients that decay at a rate $\Gamma_1(lu)$, but only those that decay at the much slower rates (in our experiments) of $\Gamma_k(l)$. In the present experiments we are concerned with only two polarizations for the pump beam, circularly polarized or linearly polarized at 45° to the magnetic-field direction. The longitudinal components of the density matrix that are generated by pump beams having either of these polarizations may be deduced from appropriate master equations for each case (see the Appendix). Those equations show that with a circularly polarized pump beam $\rho_0^1(l)$, $\rho_0^2(l)$, $\mathrm{Re}\rho_1^1(l)$ and $\mathrm{Re}\rho_2^2(l)$ are generated, but $\mathrm{Im}\rho_1^2(l)$ is not, while with a 45° linearly polarized pump $\rho_0^2(l)$, $\mathrm{Im}\rho_1^2(l)$, and $\mathrm{Re}\rho_2^2(l)$ are generated, but $\mathrm{Re}\rho_1^1(l)$ is not. Thus for the case of a probe beam polarized in the y direction Eqs. (4) and (7) predict that, for a circularly polarized pump,

$$(n^+-n^-)\propto-\frac{\delta+i\Gamma_1(lu)}{\Gamma_1(lu)^2+\delta^2}\mathrm{Re}\rho_1^1(l) \propto-\frac{\delta+i\Gamma_1(lu)}{\Gamma_1(lu)^2+\delta^2}e^{-\Gamma_1(l)t}\cos\omega_L t , \tag{8}$$

while for the 45° linearly polarized pump

$$(n^+-n^-)\propto-\frac{\Gamma_1(lu)-i\delta}{\Gamma_1(lu)^2+\delta^2}\mathrm{Im}\rho_1^2(l) \propto-\frac{\Gamma_1(lu)-i\delta}{\Gamma_1(lu)^2+\delta^2}e^{-\Gamma_2(l)t}\cos\omega_L t . \tag{9}$$

For these pump polarizations and a probe beam polarized in the y direction the birefringence and dichroism are not sensitive to the other lower-level density-matrix components generated, i.e., $\rho_0^1(l)$, $\rho_0^2(l)$, or $\mathrm{Re}\rho_2^2(l)$. This means that the signal transmitted through the nearly crossed polarizers has the form [from Eqs. (1) and (9)]

$$I\propto\theta^2+a_1\theta e^{-\Gamma_k(l)t}\cos\omega_L t+a_2 e^{-2\Gamma_k(l)t}\cos^2\omega_L t , \tag{10}$$

where $k=1$ applies for a circularly polarized pump, in which case

$$a_1\propto-\frac{\delta}{\Gamma_1(lu)^2+\delta^2},\quad 4a_2=a_1^2+\frac{\Gamma_1(lu)^2}{[\Gamma_1(lu)^2+\delta^2]^2} ,$$

and $k=2$ applies for a 45° linearly polarized pump, with

$$a_1\propto-\frac{\Gamma_1(lu)}{\Gamma_1(lu)^2+\delta^2},\quad 4a_2=a_1^2+\frac{\delta^2}{[\Gamma_1(lu)^2+\delta^2]^2} .$$

For the bulk of the experiments θ was sufficiently large that the first two terms in Eq. (10) dominate the quadratic term. The experimental traces therefore show beat patterns almost symmetrical about a constant background level (proportional to θ^2), modulated at ω_L, and decaying exponentially at a rate $\Gamma_k(l)$.

For the case of a circularly polarized pump beam the transmitted intensity has a dispersion-shaped dependence on δ, while for the linearly polarized case the dependence is Lorentzian. Although the above expressions have been derived for the single atomic velocity group for which the laser-atom detuning is δ, it can be readily appreciated that after the entire atomic velocity distribution is considered, the maximum signal for a circularly polarized pump laser occurs when the probe laser frequency is detuned away from exact atomic resonance by an amount comparable to the Doppler width, while for the linearly polarized case the signal is strongest when the probe laser is exactly on resonance.

The preceding arguments involved setting $\beta=\pi/2$, the probe polarization angle used for most of the experiments in the present work. It should be noted that choosing $\beta=0$, i.e., probe polarization parallel to the magnetic-field direction, would have allowed similar arguments to be applied and the same quantities to be measured. If the polarization of the probe beam is other than normal or parallel to the magnetic-field direction then the transmitted signal will be sensitive to $\rho_0^2(l)$ and $\mathrm{Re}\rho_2^2(l)$ as well as $\mathrm{Re}\rho_1^1(l)$ or $\mathrm{Im}\rho_1^2(l)$. This is discussed further in Sec. IV A, as is the case of exactly crossed polarizers ($\theta=0$) for which only the quadratic term in Eq. (10) is nonzero.

The theory outlined in this section is appropriate to a $J_l=1$ to $J_u=0$ probe transition. Applying the theory to transitions with higher J values yields more complicated but essentially similar results.

III. EXPERIMENT

The experimental arrangement used for recording transmission Zeeman beats is shown in Fig. 1. The pump laser was a nitrogen-laser pumped dye laser (pulse duration 4 ns, bandwidth 20 GHz) and the probe laser an actively stabilized cw dye laser (bandwidth 1 MHz). The pump beam was first polarized at 45° to the magnetic-field direction and the polarization of the beam entering the cell was adjusted to be either linear (45° to magnetic-field direction) or circular by means of the Babinet-Soleil compensator. The probe beam for most of the experiments was linearly polarized normal to the magnetic-field direction. After traversing the vapor cell the probe beam passed through the nearly crossed analyzer P2 and after suitable attenuation was detected by the photomultiplier. The extinction coefficient of the polarizers was about 10^{-4}. The beat signals were recorded by a fast transient digitizer (bandwidth 500 MHz) that was triggered from the pump-laser pulses. The probe beam diameter was normally around 5 mm and the intensity was sufficiently weak (typically 5 mW cm^{-2} for Sm 570.68 nm) not to affect the measured decay rates. The intensity of the pump pulses was typically 30 kW cm^{-2}.

The samarium vapor was produced by cathodic sputtering in a rare-gas discharge, using a demountable glass cell similar to that described previously.[20] The cathode consisted of a flat piece of samarium metal welded to a strip of zirconium of area about 0.5 cm^2. For all measurements (except those for Sm $^7F_1$ in helium) the discharge was operated in a pulsed mode at a repetition rate of about 20 Hz, with discharge currents of typically several milliamps, depending on the pressure of rare gas. Under these conditions the cathode sometimes became sufficiently hot that the samarium vapor originated from both thermal evaporation and cathodic sputtering. However, the sputtering discharge was essential for populating the higher-lying levels in the $4f^6 6s^2\,{}^7F$ term, which have energies up to 4000 cm^{-1} above the ground level. The beat signals were recorded following a delay of several milliseconds after each discharge pulse. This ensured that the measured relaxation rates resulted solely from rare-gas collisions and were not influenced by species produced in the discharge. For example, in the case of long-lived coherences in the $^7F_3$ and $^7F_4$ levels, the decay time of the beats was found to be shortened significantly if the measurements were made during the sputtering pulse rather than after the delay period. For all measurements the samarium atom density was controlled by adjusting the discharge current so that the absorption of the probe beam did not exceed 20%. For measurements on the 293-cm^{-1} $^7F_1$ level the temperature of the samarium vapor in the interaction region was determined from the width of Doppler-broadened fluorescence profiles obtained by scanning the frequency of the cw laser in zero magnetic field. By adjusting the position of the laser beams relative to the cathode it was possible to record the transmission beat signals at constant temperature over the range of rare-gas pressures used. For measurements on the other levels of the ^7F ground term, the temperatures were assumed to be the same as had been measured for the $^7F_1$. Background magnetic fields within the cell were compensated to less than 0.2 μT with three pairs of Helmholtz coils. The Zeeman beat signals were recorded in applied magnetic fields of 10 to 150 μT.

The various pump and probe transitions used to study the ^7F levels of Sm I are shown in Table I. The use of different transitions for the pump and probe is not essential, but in practice it was advantageous to choose probe transitions with wavelengths in the range of rhodamine 6G dye and pump transitions that allowed efficient generation of the lower-level coherence. The lower-level coherences are generated by optical pumping via a combination of absorption and stimulated and/or spontaneous emission processes, and the strongest beat signals occurred for strong pump transitions with $\Delta J=0$. The use of a strong pump transition also ensured that the lifetime of the upper level was sufficiently short (typically 7 ns) that upper-level coherences did not contribute to the transmission beat signals beyond the first few nanoseconds. It should be noted, however, that transmis-

TABLE I. Pump and probe transitions used for observation of transmission Zeeman beats in Sm I.

Level	Energy (cm^{-1})	Pump transition (nm)	Probe transition (nm)
$4f^6 6s^2\,{}^7F_1$	293	478.31($^7F_1$-$^7D_1^0$)	570.68($^7F_1$-$^7F_0^0$)
$4f^6 6s^2\,{}^7F_2$	812	476.03($^7F_2$-$^7D_2^0$)	565.99($^7F_2$-$^7F_1^0$)
$4f^6 6s^2\,{}^7F_3$	1490	472.84($^7F_3$-$^7D_3^0$)	570.62($^7F_3$-$^7G_2^0$)
$4f^6 6s^2\,{}^7F_4$	2273	468.87($^7F_4$-$^7D_4^0$)	580.28($^7F_4$-$^7F_3^0$)
$4f^6 6s^2\,{}^7F_5$	3125	471.61($^7F_5$-$^7D_5^0$)	578.84($^7F_5$-$^7F_4^0$)
$4f^6 6s^2\,{}^7F_6$	4021	429.67($^7F_6$-$^7G_7^0$)	573.29($^7F_6$-$^7F_5^0$)

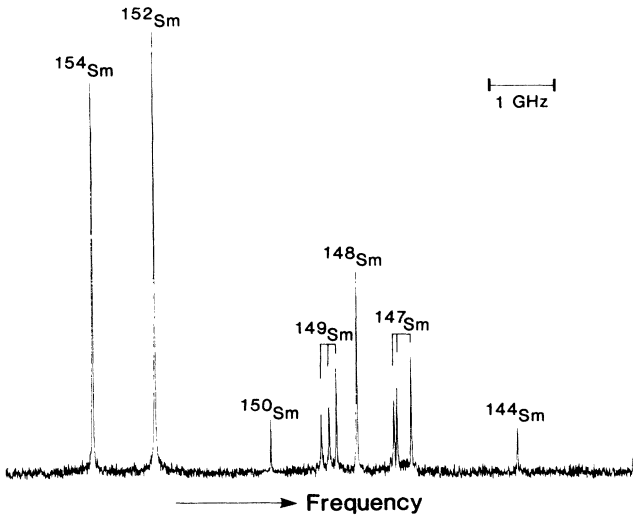

FIG. 2. Saturated absorption spectrum of Sm I 570.68-nm $^7F_1$-$^7F_0^0$ transition.

sion beat signals can also be observed in cases where the coherence is transferred solely by spontaneous emission; for example, in the 293-cm^{-1} $^7F_1$ level by pumping the $^7F_0$-$^7F_1^0$ transition at 471.71 nm and probing the $^7F_1$-$^7F_0^0$ transition at 570.68 nm. In this case, the fraction of alignment or orientation transferred from the $^7F_1^0$ upper level to the $^7F_1$ lower level by spontaneous emission is $\{^{211}_{111}\}/\{^{011}_{111}\}=1/\sqrt{2}$ and $\{^{111}_{111}\}/\{^{011}_{111}\}=1/\sqrt{2}$, respectively. Similar effects resulting from the transfer of transient coherences by spontaneous emission have previously been observed in cascade quantum beat experiments.[21]

Doppler-free saturated absorption spectra and Doppler-broadened fluorescence spectra were recorded for the various probe transitions used in this work (Table I) and in all cases the major ^{154}Sm and ^{152}Sm isotope components were found to be well resolved from the ^{147}Sm and ^{149}Sm hyperfine components in the presence of Doppler broadening. Thus, for all levels studied, the probe laser could readily be tuned to just the even isotopes ^{154}Sm or ^{152}Sm. An example of a Doppler-free scan recorded for the $^7F_1$-$^7F_0^0$ transition at 570.68 nm is shown in Fig. 2.

IV. RESULTS

A. Geometrical considerations

1. *Crossing angle of the probe beam polarizers*

Figure 3 shows transmission Zeeman beat signals recorded for the 293-cm^{-1} $^7F_1$ level when the polarizers in the probe beam are exactly crossed ($\theta=0$) and slightly uncrossed ($\theta<5°$). For the case of exactly crossed polarizers the beat pattern is determined solely by the quadratic term in Eq. (10), and the transmitted intensity of the probe is modulated at $2\omega_L$ and decays at a rate $2\Gamma_k(l)$ to a zero background level [Fig. 3(a)]. For the case of slightly uncrossed polarizers the first two terms of Eq. (10)

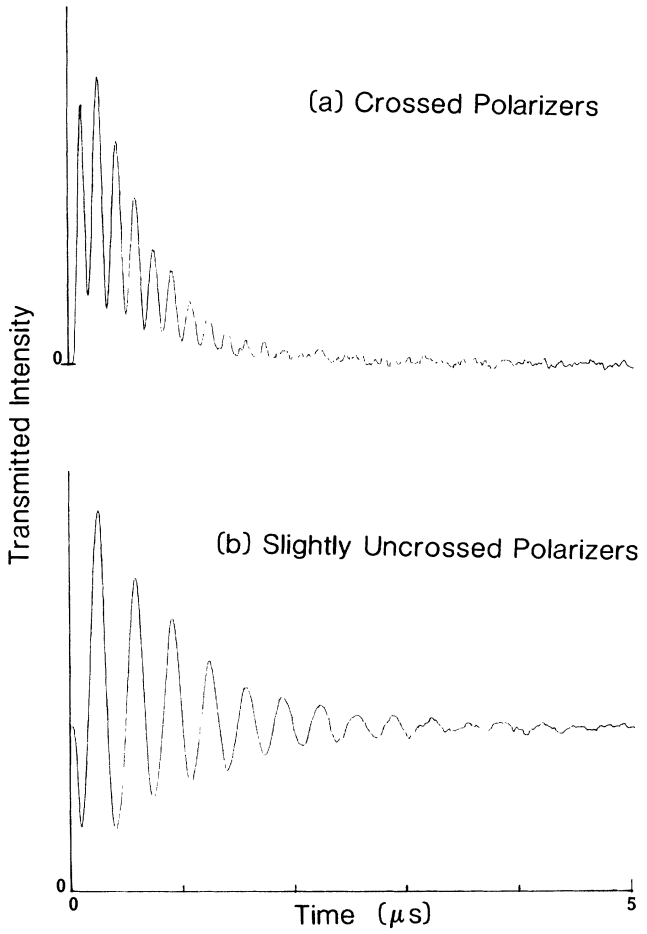

FIG. 3. Transmission Zeeman beat signals for the 293-cm^{-1} $^7F_1$ level of Sm I with (a) crossed and (b) slightly uncrossed probe beam polarizers. The pump beam is circularly polarized. The pressure is 0.5 Torr Kr. Curve (*a*) is plotted on an expanded intensity scale. The magnetic field is 150 μT.

dominate the quadratic term, and the transmitted intensity exhibits an almost symmetrical beat pattern modulated at ω_L and decaying at the rate $\Gamma_k(l)$ to a constant background intensity proportional to θ^2 [Fig. 3(b)]. The small asymmetry in this beat pattern arises from the residual contribution of the quadratic term of Eq. (10) and decreases as the uncrossing angle θ increases.

Although the beat patterns obtained with exactly crossed polarizers, which decay at $2\Gamma_k(l)$ [Fig. 3(a)], can in principle be used to measure collisional depolarization rates, we find in practice that it is difficult to avoid contributions to the signal that decay at $\Gamma_k(l)$ resulting from imperfect polarizers and background birefringence. Furthermore, the signal-to-noise ratio of the recorded beat patterns is generally worse than for the case of uncrossed polarizers. Thus we find that considerably more reliable results are obtained by uncrossing the polarizers slightly and analyzing the almost symmetrical beat patterns such as those shown in Fig. 5. For these beat signals the small asymmetry resulting from the quadratic

term of Eq. (10) is eliminated in the data analysis by analyzing the *difference* between the upper and lower envelopes of the beat pattern. For the uncrossing angles used in this work the effects on the measured relaxation rates of the quadratic term amounted to a correction of less than 10% in all cases.

2. Effect of polarization angle of the probe beam (β)

If the direction of polarization of the probe beam is other than normal or parallel to the magnetic field, then the beat pattern is influenced by other Zeeman coherence components in addition to $\mathrm{Re}\rho_1^1(l)$ and $\mathrm{Im}\rho_1^2(l)$. Equation (6) gives for any angle β

$$\mathrm{Re}(n^+-n^-)\propto\frac{1}{\Gamma_1(lu)^2+\delta^2}\left[2\delta\,\mathrm{Re}\rho_1^1(l)-2\Gamma_1(lu)\cos2\beta\,\mathrm{Im}\rho_1^2(l)+\Gamma_1(lu)\sin2\beta\left[\frac{3}{\sqrt{6}}\rho_0^2(l)+\mathrm{Re}\rho_2^2(l)\right]\right].$$

Using the solutions from the Appendix for each of these components, then for the case of a 45° linearly polarized pump such that the retardation $\phi=\pi$,

$$\mathrm{Re}(n^+-n^-)\propto e^{-\Gamma_2(l)t}[4\cos2\beta\cos\omega_L t+\sin2\beta(\cos2\omega_L t-1)]\ .$$

This expression is plotted in the right-hand column of Fig. 4 for $\beta=0°$, 30°, 45°, 60°, and 90°, alongside corresponding experimental profiles. The influence of the components $\rho_0^2(l)$ and particularly $\mathrm{Re}\rho_2^2(l)$, whose contribution to the signal is modulated at twice the Larmor frequency, is observable at the intermediate probe polarization angles. Indeed, the curves for $\beta=45°$ contain only contributions from $\rho_0^2(l)$ and $\mathrm{Re}\rho_2^2(l)$.

B. Collisional depolarization in the $4f^6 6s^2\,{}^7F_1$ level

Figure 5 shows transmission beat signals obtained for the Sm $^7F_1$ level in the presence of argon for the cases of circular and linear (45°) pump beam polarizations. A significant difference in the collisional relaxation rates for the two polarizations is clearly evident. Relaxation rates measured as a function of rare-gas pressure (see, for example, Fig. 3 of Ref. 9), have been used to derive the cross sections for collisional destruction of orientation (σ_1) and alignment (σ_2) in each of the rare gases He, Ne, Ar, Kr, and Xe. The results are summarized in Table II along with cross sections obtained previously from radio-frequency laser double-resonance experiments,[22] collision-induced Ramsey resonance experiments,[23] and

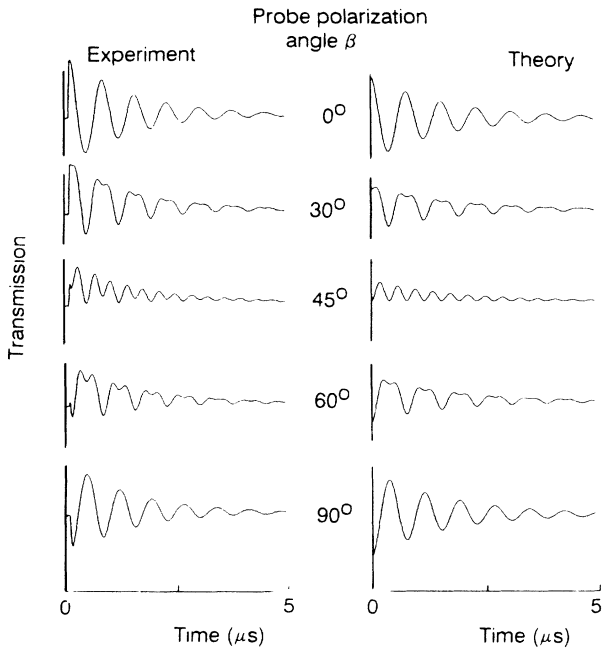

FIG. 4. Effect of angle of polarization of probe beam on transmission Zeeman beat signals. (a) Experiment, 45° linearly polarized pump. Probe polarizers slightly uncrossed. The pressure is 0.9 Torr Ne. The magnetic field is 64 μT. (b) Theory, assuming decay time 1.7 μs.

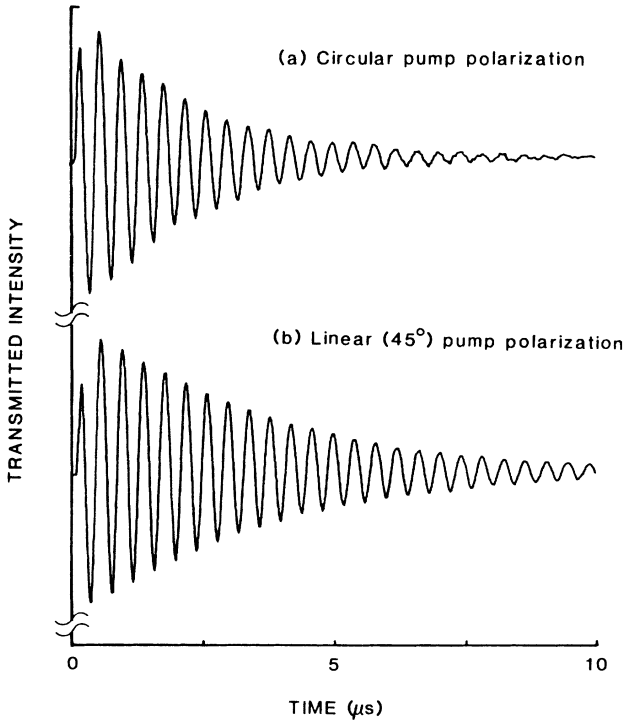

FIG. 5. Experimental transmission Zeeman beat signals recorded for the 293-cm^{-1} $^7F_1$ level of Sm I at a pressure of 0.25 Torr Ar. The magnetic field is 120 μT. Signals represent average of 640 pump laser pulses over 30 s.

TABLE II. Cross sections (Å^2) for destruction of orientation (σ_1) and alignment (σ_2) in the $4f^6 6s^2\,{}^7F_1$ level of Sm I by rare-gas perturbers. Hard-sphere collision cross sections (σ_{HS}) are also shown.

	This work[a]			Other work			
Perturber	σ_1	σ_2	σ_1/σ_2	σ_2	σ_1		σ_{HS}
He	1.5(2)	0.96(5)	1.58(22)	1.4[b]	0.025[c]	1.8[d]	28[e]
Ne	6.8(3)	4.3(2)	1.59(11)	5.3[b]		10[d]	30[e]
Ar	16.1(8)	10.3(5)	1.56(11)	12.0[b]	0.31[c]	21[d]	36[e]
Kr	27(1)	17.0(9)	1.61(11)			32[d]	41[e]
Xe	32(2)	20.6(1.0)	1.56(11)	16.0[b]	0.82[c]	40[d]	47[e]

[a]Temperature 515 K (He 545 K).
[b]Reference 22. Radio-frequency-laser double resonance. Temperature 1000 K.
[c]Reference 11. Collision-induced Hanle resonances in four-wave mixing. Temperature 1130 K.
[d]Reference 23. Collision-reduced Ramsey resonances. Temperature 1000 K.
[e]Data quoted in Ref. 22.

collision-induced Hanle resonances in four-wave mixing.[11] Our results show general agreement with those of Tamm, Buhr, and Mlynek[22] for σ_2 and Buhr and Mlynek[23] for σ_1, but are very much larger than the collision-induced Hanle results of Zou and Bloembergen[11] for σ_1. In the latter technique, the measurements were made at large detunings ($\approx$20 GHz) from line center of the $^7F_1$-$^7F_0^0$ resonance at 570.68 nm and it has been suggested[11,23] that the very small cross section reported in Ref. 11 may have been influenced by the nearby strong transition at 570.62 nm ($^7F_3$-$^7G_2^0$) or the weaker 570.72 nm ($^7F_2$-$^7I_3^0$) transition. Our very small cross sections for collisional destruction of orientation in the $^7F_2$ and $^7F_3$ levels of Sm I (Table III) support this interpretation.

The ratios of the cross sections σ_1/σ_2 obtained in this work for the $^7F_1$ level (Table II) are found to be essentially the same (in the range 1.56–1.61) for all the rare gases. The ratios deduced from the results of Tamm, Buhr, and Mlynek[22] and Buhr and Mlynek[23] range from 1.3 (He) to 2.5 (Xe), but these values were determined from data taken using different experimental techniques for σ_1 and σ_2.

C. Collisional depolarization in $4f^6 6s^2\,{}^7F$ levels with $J > 1$

The transmission beat signals for the $J=2$ to 6 levels of the ^7F ground-level term were recorded using the pump and probe transitions listed in Table I. The derived cross sections for collisional destruction of orientation and alignment by argon are given in Table III. The cross sections show very large variations (a factor of 160 for σ_1) across the various term members, with a systematic decrease from $J=1$ to 4 followed by an increase for $J=5$ and 6. An example of the very long relaxation times recorded for the $^7F_4$ level is shown in Fig. 6, where the beats are seen to persist clearly for more than 0.2 ms after the pump pulse. For the long-lived coherences in the $^7F_3$ and $^7F_4$ levels the observed relaxation rates at low pressures are influenced by the transit times of the coherently prepared Sm atoms across the probe beam, and in order to reduce such effects the probe beam was expanded from its normal 5 mm diameter to about 15 mm. The residual transit-time effects show up as a nonlinearity at the low-pressure end of the relaxation rate versus pressure plots (see Fig. 7). The cross sections given in Table III are derived from the linear (higher-pressure) region of these plots. Our measured cross section for the destruction of orientation in the $^7F_3$ level of only 0.19(2) Å^2 is in fair agreement with the value of 0.34 Å^2 reported by Buhr and Mlynek[23] from collision-induced Ramsey resonance experiments.

For levels having $J > 1$ it is possible in principle to induce higher-order coherences with $k > 2$. Such coherences would decay at a rate Γ_k, which may be different

TABLE III. Cross sections (Å^2) for destruction of orientation (σ_1) and alignment (σ_2) in ground-level term levels of samarium by argon perturbers. Also shown are the ratios of the geometrical factors $\Phi_{1,2}/\Phi_{2,2}$ (from Table V) and the modified cross sections λ.

	Energy	This work			Theory	λ
Level	(cm^{-1})	σ_1	σ_2	σ_1/σ_2	$\Phi_{1,2}/\Phi_{2,2}$	(Å^2)
$4f^6 6s^2\,{}^7F_1$	293	16.1(8)	10.3(5)	1.56(11)	1.67	16.1(8)
$4f^6 6s^2\,{}^7F_2$	812	2.2(2)	5.2(5)	0.42(4)	0.41	11(1)
$4f^6 6s^2\,{}^7F_3$	1490	0.19(2)	0.48(5)	0.39(5)	0.37	2.7(3)
$4f^6 6s^2\,{}^7F_4$	2273	0.10(1)	0.22(2)	0.46(5)	0.35	3.0(3)
$4f^6 6s^2\,{}^7F_5$	3125	0.77(9)	1.8(2)	0.42(7)	0.35	42(5)
$4f^6 6s^2\,{}^7F_6$	4021	1.7(3)	4.3(6)	0.39(9)	0.34	155(30)

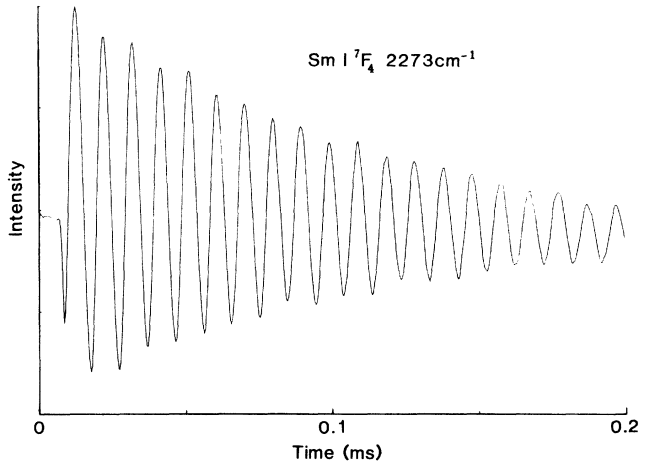

FIG. 6. Transmission Zeeman beat signal recorded for the 2273-cm^{-1} $^7F_4$ level of Sm I at a pressure of 0.5 Torr Ar, with circular pump polarization. The magnetic field is 5 μT.

from Γ_1 or Γ_2, and would evolve at various multiples of the Larmor frequency. In the present experiments the signals are not directly sensitive to such higher-order coherences, though the pump field may in principle couple them to coherences that do directly influence the signals. However, no evidence of such effects was observed for the pump-laser intensities and pulse lengths employed in these experiments.

D. Collisional depopulation rates

As mentioned in Sec. II, the collisional depolarization cross sections σ_k may consist of two contributions: one from collisions that only mix the Zeeman states (Λ_k) and another from collisions that remove population from the level (σ_0). In order to estimate the contribution of depopulation to the measured ^7F_J depolarization cross sections, we have carried out additional experiments in which the pulsed laser was used to induce a sudden change in the population of a selected lower level by spontaneous emission from a short-lived laser-excited level, using an excitation sequence such as that illustrated in Fig. 8. The decay of this laser-induced population change was then monitored by measuring the time-dependent absorption of the probe laser in the absence of the analyzing polarizer. The measured depopulation times were found to be very similar for all of the $4f^6 6s^2\,^7F$ levels and to correspond approximately to the transit times estimated from the beats experiments (see, for example, the low-pressure end of Fig. 7). Also, the depopulation times decreased when the size of the probe beam was reduced, further indicating that these measurements were dominated by transit-time effects. These results indicate that any collisional depopulation of the lower levels occurs more slowly than transit-time effects and hence does not contribute significantly to the measured depolarization cross sections. Thus for all the samarium $4f^6 6s^2\,^7F_J$ levels, σ_k can be taken as equal to Λ_k.

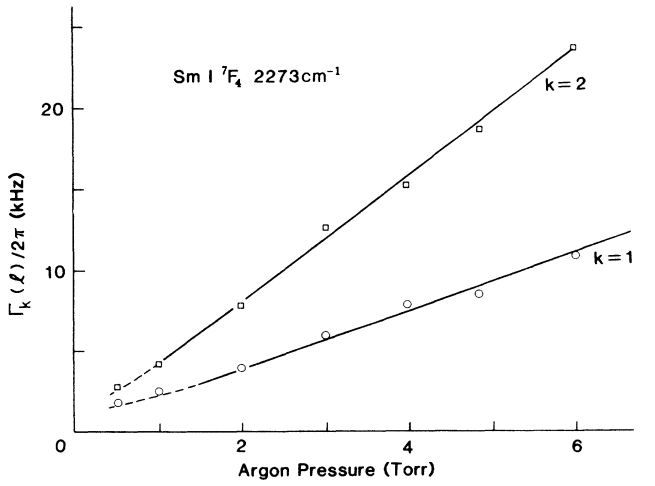

FIG. 7. Argon pressure dependence of measured depolarization rates $\Gamma_1(l)$ and $\Gamma_2(l)$ for the 2273-cm^{-1} $^7F_4$ level of Sm I.

E. Collisional transfer of coherence

The transmission Zeeman beats technique also permits studies of collisional transfer of coherence that may occur between the samarium levels as a result of the samarium–rare-gas collisions. Similar effects are well known in optical pumping experiments in ^{3}He[24] and Hanle-effect experiments on excited levels.[25] In an experiment to detect collisional transfer of coherence, the probe beam was tuned to a transition from a lower level that is not directly populated by either spontaneous or stimulated emission from the level excited by the pump laser pulse. Figure 9 shows an example of weak transmission beats detected with the pump laser tuned to the 472.84-nm $^7F_3$-$^7D_3^0$ transition and the probe laser tuned to the 570.68-nm $^7F_1$-$^7F_0^0$ transition. The observed relaxation rate of these beats (detected in the $^7F_1$ level) is similar to the measured relaxation rate of beats detected when probing from the $^7F_3$ level directly and indicates

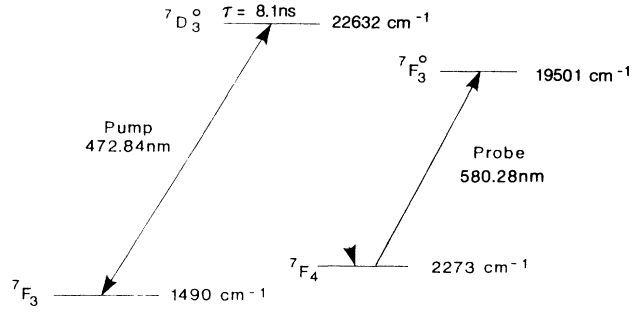

FIG. 8. Excitation scheme to study the collisional rate of change of population in the 2273-cm^{-1} $^7F_4$ level of Sm I. Dashed line represents spontaneous emission. Lifetime of $^7D_3^0$ level from Ref. 42.

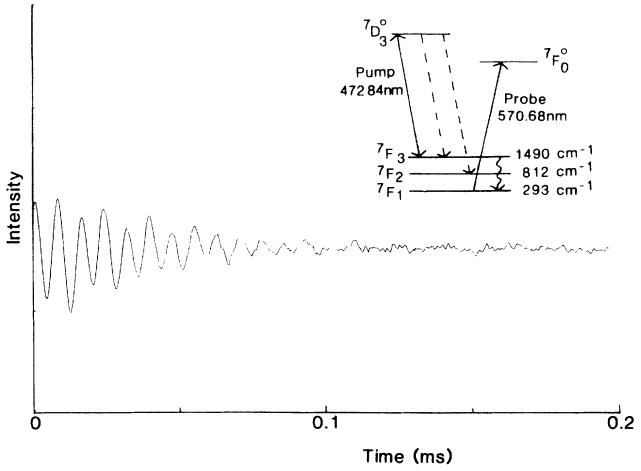

FIG. 9. Transmission Zeeman beats recorded for the 293-cm^{-1} $^7F_1$ level of Sm I following collisional transfer of coherently excited atoms from the 1490-cm^{-1} $^7F_3$ level. The pressure is 0.5 Torr Ar. The pump polarization is circular. The magnetic field is 7 μT. Dashed lines of inset represent spontaneous emission and wavy line represents collisional transfer.

that the coherence detected in the $^7F_1$ level has been transferred from $^7F_3$ to $^7F_1$. In particular, this relaxation rate precludes possible alternative mechanisms such as spontaneous emission from $^7D_3^0$ to $^7F_2$ followed by collisional transfer from $^7F_2$ to $^7F_1$, or collisional transfer among the short-lived excited levels followed by spontaneous emission to the $^7F_1$ level. Weak collisionally induced coherence transfer beats have also been detected by probing the $^7F_2$-$^7F_1^0$ transition following pumping on a $J_l=1$ to $J_u=0$ transition. In these experiments we have not determined the degree of coherence transfer, but it must be very small since the population changes accompanying such a transfer are not detected (Sec. IV D). Furthermore beats detected when probing from the $^7F_2$ level with the pump laser tuned to the $^7F_3$-$^7D_3^0$ transition have relaxation rates corresponding to just $J_l=2$ coherences and show no detectable influence from the much longer-lived $^7F_3$ coherences.

V. DISCUSSION

The cross sections for collisional depolarization in the samarium $4f^6 6s^2\,^7F_{1-6}$ levels by the rare gases exhibit a number of significant trends (Tables II and III). First, they appear to be unusually small compared with the depolarization cross sections for other $J \geq 1$ levels studied to date (see, for example, Refs. 26 and 27) and with the cross sections for hard-sphere collisions (Table II). Second, the depolarization cross sections show a strong monotonic increase with rare-gas perturber from helium through to xenon (Table II). Such behavior resembles that found for weak depolarizing collisions in the $^2S_{1/2}$ ground levels of alkali-metal atoms (see, for example, Ref. 28). Third, the cross sections vary markedly (by factors of up to 160) from level to level within the ^7F term (Table III), and finally, the cross sections for destruction of orientation in the case of the $^7F_1$ level are considerably higher than the cross sections for destruction of alignment ($\sigma_1/\sigma_2=\Lambda_1/\Lambda_2=1.56-1.61$ for the various rare-gas perturbers), while for the higher-J ^7F levels the reverse is true (σ_1/σ_2 in the range 0.39–0.46 for argon perturbers). The σ_1/σ_2 ratios for the $^7F_1$ level are considerably higher than those for other $J=1$ levels studied previously, where values in the range of $\sigma_1/\sigma_2=1.03-1.33$ have been found in Hg $6\,^3P_1$,[29,30] Cd $5\,^1P_1$,[31] Cd $5\,^3P_1$,[32] Yb $6\,^3P_1$,[17] and Ne $2s_2$ ($J=1$),[33] all of which are in reasonable agreement with the detailed numerical calculations of Berman and Lamb[34] ($\sigma_1/\sigma_2=1.12\pm0.02$) and the perturbative calculations of Omont[35] ($\sigma_1/\sigma_2=1.11$).

The (velocity-averaged) cross section for collisional relaxation of the 2^k multipole is given in the impact approximation by (for example, Refs. 27 and 36)

$$\sigma_k=\bar{v}^{-1}\int_0^\infty\int_0^\infty f(v)2\pi\left[1-\sum_{\chi,\sigma}(-1)^{2J+k+\chi}\begin{Bmatrix}J & J & k\\ J & J & \chi\end{Bmatrix}|S_\sigma^\chi(b,v)|^2\right]bdb\,vdv\ , \tag{11}$$

where $S_\sigma^\chi(b,v)$ are irreducible components of the scattering S matrix for a collision having impact parameter b and relative velocity v, and $f(v)$ is the atomic velocity distribution. It is useful to express Eq. (11) explicitly as an expansion in terms of the multipolarities χ of the collision interaction:[37]

$$\Lambda_k=\sigma_k-\sigma_0=\sum_{\chi=1}^{2J}\Phi_{k,\chi}B_\chi\ , \tag{12}$$

where

$$\Phi_{k,\chi}=2\left[(2J+1)^{-1}-(-1)^{2J+k+\chi}\begin{Bmatrix}J & J & k\\ J & J & \chi\end{Bmatrix}\right] \tag{13}$$

is a geometrical factor and the coefficients B_χ are given by

$$B_\chi=(2\bar{v})^{-1}\int_0^\infty\int_0^\infty f(v)2\pi\sum_\sigma|S_\sigma^\chi(b,v)|^2bdb\,vdv\ . \tag{14}$$

Expressions similar to (12) and (13) have also been given by Happer[38] for the case of an interaction with a single multipolarity χ.

Equations (12) and (13) lead to the following relationship for the ratios of the cross sections for the destruction of orientation and alignment:

$$\frac{\Lambda_1}{\Lambda_2}=\frac{\Phi_{1,\chi}}{\Phi_{2,\chi}}=\frac{(2J-1)(2J+3)\sum_{\chi=1}^{2J}\chi(\chi+1)B_\chi}{3\sum_{\chi=1}^{2J}\chi(\chi+1)[4J(J+1)-\chi(\chi+1)-1]B_\chi}\ , \tag{15}$$

from which one obtains the inequalities[37]

$$(2J+3)/3 \geq \Lambda_1/\Lambda_2 \geq \tfrac{1}{3}\ , \tag{16}$$

where the lower limit corresponds to a pure $\chi=1$ interaction only and the upper limit corresponds to a pure $\chi=2J$ interaction.

In the case of a $J=1$ level ($k=1,2$ and $\chi=1,2$ only), expression (16) yields $\frac{5}{3}$ (pure $\chi=2$) $\geq \Lambda_1/\Lambda_2 \geq \frac{1}{3}$ (pure $\chi=1$). The upper limit $\Lambda_1/\Lambda_2=\frac{5}{3}$ is the same as the ratio given by Omont[35] and Wang and Tomlinson[39] when noncommutativity of the interaction matrix is neglected, and is very close to our experimentally determined $\sigma_1/\sigma_2(=\Lambda_1/\Lambda_2)$ values of 1.56–1.61 for the $^7F_1$ level of samarium. Indeed, the values of the B_χ coefficients obtained when the experimental values of σ_1 and σ_2 are substituted into Eq. (12) (see Table IV) indicate that for this level the contribution to the sum in Eq. (12) from the $\chi=1$ component is less than 6%, which is smaller than the experimental uncertainty. Thus the collision interaction is dominated by a $\chi=2$ (electric quadrupole) interaction.

In the case of a $J=2$ level ($\chi=1$, 2, 3, or 4) the limiting values of Λ_1/Λ_2 are $\frac{7}{3}$ (pure $\chi=4$) $\geq \Lambda_1/\Lambda_2 \geq \frac{1}{3}$ (pure $\chi=1$), while the ratio for a pure $\chi=2$ interaction is $\Lambda_1/\Lambda_2=\Phi_{1,2}/\Phi_{2,2}=\frac{7}{17}=0.41$, which is in agreement with our experimentally determined value (0.42 ± 0.04) for the $^7F_2$ level of samarium. Likewise, in the case of $J=3$–6 levels, the values of $\Phi_{1,2}/\Phi_{2,2}$ (i.e., $\chi=2$ interaction) are consistent with the experimentally determined σ_1/σ_2 values for the $^7F_{3-6}$ levels of Sm (see Table III). Theoretical ratios of Λ_1/Λ_2 for $\chi=1$, 2, 3, and 4 are compared with the experimental ratios in Fig. 10. These results show that collisional depolarization for all $J\geq 1$ levels in the $4f^6 6s^2\,^7F$ term of samarium appears to be dominated by a $\chi=2$ interaction, in which case the J dependence of the ratios of the cross sections [Eq. (15)] is given by

$$\frac{\Lambda_1}{\Lambda_2}=\frac{(2J-1)(2J+3)}{3[4J(4J+1)-7]}\ . \tag{17}$$

An essentially pure quadrupole collision interaction has previously been found in optical pumping experiments on polarized ground-state atoms of ^{201}Hg($6\,^1S_0, F=\frac{3}{2}$) (Ref. 40) and ^{109}Cd($5\,^1S_0, F=\frac{5}{2}$).[41] In these cases the interaction is between the quadrupole moment of the atomic nucleus and fluctuating electric-field gradients experienced by the atoms in collisions with the walls of the cells.

TABLE IV. Values of the coefficients B_χ (in Å^2) for the $4f^6 6s^2\,^7F_1$ level, deduced from the experimental values of σ_1 and σ_2 (Table III) and Eq. (12).

Perturber	B_1	B_2
He	0.08(16)	1.5(3)
Ne	0.28(34)	6.7(4)
Ar	0.8(9)	15.8(1.0)
Kr	1.0(1.4)	27(1)
Xe	1.8(2.8)	31(3)

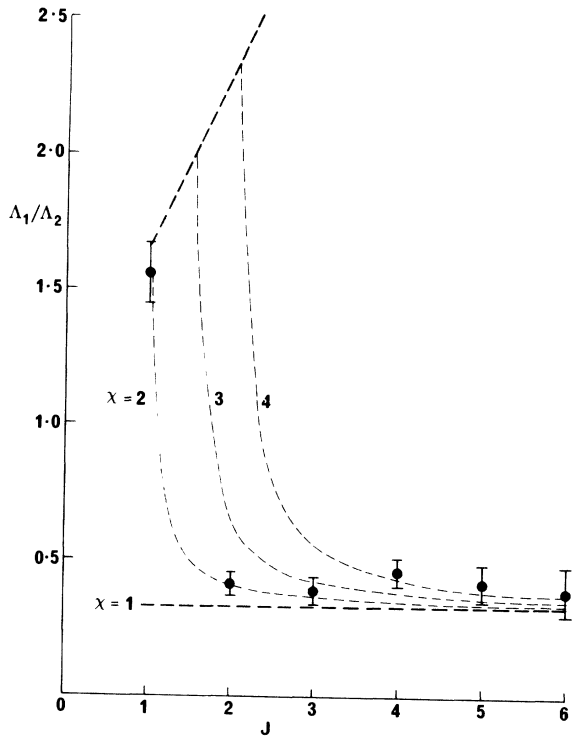

FIG. 10. Ratio Λ_1/Λ_2 plotted as a function of J. Dashed curves join theoretical values assuming single multipolarity interaction, for $\chi=1$, 2, 3, and 4. Closed circles indicate experimentally determined ratios for samarium $4f^6 6s^2\,^7F$ levels with argon perturbers. Heavy dashed lines represent limits given by expression (16).

It is interesting to note that the observation of $\Lambda_1/\Lambda_2=\frac{5}{3}$ for $J=1$, corresponding to a pure $\chi=2$ interaction, implies that the cross section for population transfer between the $m=1$ and -1 substates is just twice that for transfer between the $m=1$ (or -1) and $m=0$ substates.[39] Similarly, using Eq. (A5) of Ref. 39, observed values of $\Lambda_1/\Lambda_2=\frac{7}{17}$ for $J=2$ and $\Lambda_1/\Lambda_2=\frac{15}{41}$ for $J=3$, corresponding to a pure $\chi=2$ interaction, imply the relative population transfer cross sections given in Fig. 11. We note that for a $\chi=2$ interaction the sum of the cross sections for $\Delta m=\pm1$ collisions is always the same as the sum of the cross sections for $\Delta m=\pm2$ collisions, while collisions in which m changes by more than 2 are not allowed.

As J becomes large the final term in Eq. (13), involving the 6-j symbol, approaches $(2J+1)^{-1}$, so that the geometrical factor $\Phi_{k,\chi}$ approaches zero. This J dependence of $\Phi_{k,\chi}$ (Table V) is found to account for much of the large decrease in the experimental σ_1 and σ_2 values (Table III) as J increases from 1 to 4. It is useful to derive a modified cross section λ which does not contain the J dependence of the geometrical factor $\Phi_{k,\chi}$. For $k=1$ Eqs. (12) and (13) reduce to the simple expression

$$\Lambda_1=[J(J+1)(2J+1)]^{-1}\sum_{\chi=1}^{2J}\chi(\chi+1)B_\chi\ , \tag{18}$$

and we define

TABLE V. Values of the geometrical factor $\Phi_{k,2}$, defined by Eq. (13), for $k=1,2$ and $J=1-6$.

J	$\Phi_{1,2}$	$\Phi_{2,2}$
1	1	$\frac{3}{5}$
2	$\frac{1}{5}$	$\frac{17}{35}$
3	$\frac{1}{14}$	$\frac{41}{210}$
4	$\frac{1}{30}$	$\frac{73}{770}$
5	$\frac{1}{55}$	$\frac{113}{2145}$
6	$\frac{1}{91}$	$\frac{23}{715}$

$$\lambda=\tfrac{1}{6}J(J+1)(2J+1)\Lambda_1=\tfrac{1}{6}\sum_{\chi=1}^{2J}\chi(\chi+1)B_\chi\ . \qquad (19)$$

Equation (19) permits λ to be determined from the experimental σ_1 ($=\Lambda_1$) values without prior knowledge about which values of χ contribute to the interaction. These λ values, given in Table III, indicate that after allowing for the J dependence of $\Phi_{k,\chi}$ the higher-lying $^7F_5$ and $^7F_6$ levels are much more susceptible to collisional depolarization than the lower-lying $^7F_{1-4}$ levels. The $^7F_5$ and $^7F_6$ levels were also found to be quite sensitive to depopulation by discharge species during the current pulse.

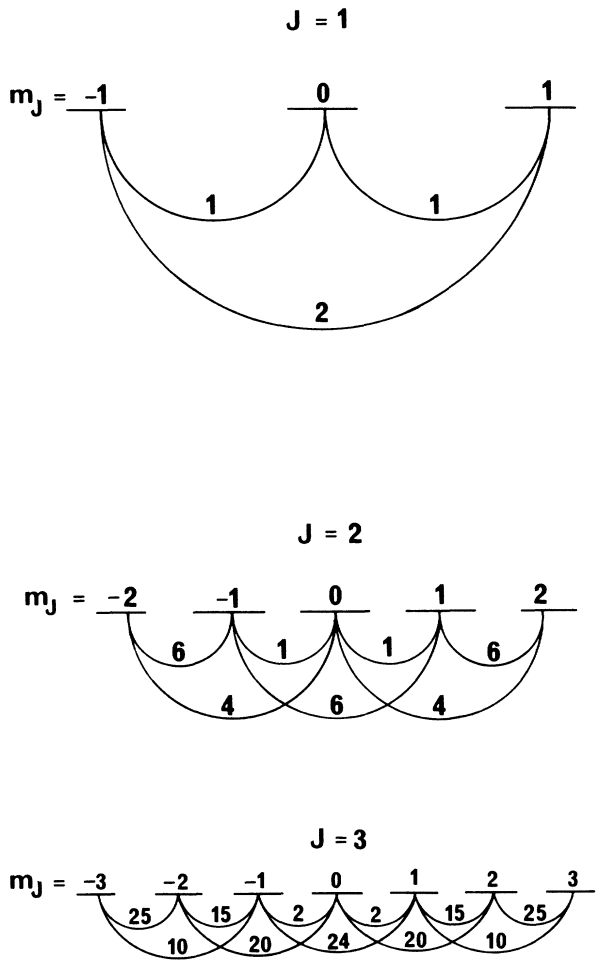

FIG. 11. Relative collisional population transfer cross sections between Zeeman states of levels having $J=1$, 2, and 3 for a pure $\chi=2$ interaction.

The occurrence of an essentially pure even-χ interaction for collisional depolarization in the samarium $4f^6 6s^2\,^7F$ levels by the rare gases is in contrast with other $J\geq 1$ systems reported to date; particularly, $J=1$ levels, in which the ratio Λ_1/Λ_2 is very sentitive to the contribution each multipolarity χ makes to the sum in Eq. (12). A pure even-χ interaction implies that, in the expansion of the scattering S matrix, second- and higher-order terms that contain commutators $[\mathbf{V}(t_1),\mathbf{V}(t_2)]$ of the collision interaction matrix $\mathbf{V}(t)$ can be ignored at all times during the collision.[27,43] Such a situation arises in a weak collison interaction or when the commutators vanish due to symmetry considerations as in depolarizing collisions between $^2S_{1/2}$ ground-state alkali-metal atoms and $^1S_0$ ground-state rare-gas perturbers. In the case of samarium the unusual but simple behavior of the collisional depolarization in the $4f^6 6s^2\,^7F$ levels is likely to be a consequence of the strong screening action of the $5s$, $5p$, and $6s$ shells on the $4f$ valence electrons. Such strong screening is also reflected in the relatively small absolute values of the depolarization cross sections of the levels (Table III) and their very small collisional mixing or depopulation rates (Sec. IV D). Evidence for this screening is also found in the abnormally small pressure-broadening constants found for $M1$ transitions between the samarium $4f^6 6s^2\,^7F_J$ levels[44] and for optical $M1$ transitions between levels in different terms within the $4f^6 6s^2$ configuration.[45] Very small pressure-broadening constants have also been found for thulium $M1$ transitions between $4f^{13}6s^2\,^7F_{5/2,3/2}$ fine-structure levels.[46] Behavior similar to that which we have observed in samarium could be expected in ground-level terms of other rare-earth and actinide atoms.

VI. SUMMARY

The transmission Zeeman beat technique described in this paper has been shown to provide an accurate means of determining depolarization rates in ground and near-ground atomic levels. With an appropriate choice of polarization of the pump laser, the technique yields individual relaxation rates for the destruction of either orientation or alignment. Since the depolarization rates are determined directly from the decay of the Zeeman beat signals, they should yield inherently more accurate cross sections than other measurements of ground-level depolarization rates which rely on the fitting of more than one parameter to complex linewidth-versus-pressure curves (e.g., see Refs. 11, 22, and 23) or the measurement of narrow linewidths that may be susceptible to extraneous broadening. In particular, the present technique is not affected by relaxation processes associated with velocity-changing collisions since the pump-laser bandwidth is greater than the Doppler width. The principal source of uncertainty in the present experiments has been the difficulty of accurately measuring the temperature of the atomic vapor in the discharge.

The application of the transmission Zeeman beat tech-

nique to levels in the $4f^6 6s^2\,{}^7F$ ground-level term of samarium has yielded a number of significant results. First, the small depolarization rates found in these levels makes this system particularly attractive for experiments requiring narrow ground-state resonances, such as some ground-state Hanle-effect and optical pumping experiments. Furthermore, the samarium ground-level term has proved to be a useful test case for studying the nature of the collision interaction in levels having a wide range of J values. In the case of the ${}^7F_1$ level, the cross sections for the destruction of orientation in collisions with rare-gas atoms are considerably larger than the alignment-destroying cross sections, whereas for the ${}^7F_{2-6}$ levels the alignment-destroying cross sections are the larger. These results are in quantitative agreement with the predictions of a weak collision model based on a pure $\chi=2$ collisional interaction. The observation of values of $\sigma_1/\sigma_2\approx 1.6$ for the ${}^7F_1$ level is believed to be the first observation of the ratio close to the theoretical result of $\frac{5}{3}$ predicted by the above simple model.

ACKNOWLEDGMENTS

We wish to express our gratitude to D. S. Gough, who made a substantial contribution to the early stages of these experiments, to E. L. Lewis for bringing to our attention the significance of the ratio $\sigma_1/\sigma_2=\frac{5}{3}$ for a $J=1$ level, and to W. E. Baylis for generously providing a theoretical treatment of relaxation of atomic polarization in atomic collisions in a personal communication.

APPENDIX: ZEEMAN COHERENCES GENERATED BY THE PUMP LASER

The pump beam is initially linearly polarized in the xy plane at 45° to the direction of the magnetic field, and propagates through the Babinet-Soleil compensator, acting as a wave plate, with its fast axis vertical. The retardation induced in the component of the wave polarized along the slow axis is ϕ. Although the pump laser is broadband, with a pulse length of about 4 ns, we are concerned here primarily with establishing which Zeeman coherences are generated by the pump pulse. We use the following equations describing the steady-state interaction of a single atomic velocity group (for which $\delta=0$) with a single mode of a pump laser field, and ignore the effects of the magnetic field ($\omega_L=0$):

$$\left[\frac{\Gamma_1(lu)\Gamma_1(l)}{\Omega^2}+\frac{1}{4}\right]\mathrm{Re}\rho_1^1(l)$$
$$=\frac{1}{\sqrt{3}}\sin\phi\rho_0^0(l)-\frac{1}{8\sqrt{6}}\sin\phi\rho_0^2(l)$$
$$+\frac{1}{8}\sin\phi\,\mathrm{Re}\rho_2^2(l)-\frac{1}{4}\sin\phi\ ,$$

$$\left[\frac{\Gamma_1(lu)\Gamma_2(l)}{\Omega^2}+\frac{5}{24}\right]\rho_0^2(l)$$
$$=\frac{1}{3\sqrt{2}}\rho_0^0(l)-\frac{1}{4\sqrt{6}}\sin\phi\,\mathrm{Re}\rho_1^1(l)$$
$$-\frac{1}{4\sqrt{6}}\cos\phi\,\mathrm{Im}\rho_1^2(l)-\frac{1}{4\sqrt{6}}\mathrm{Re}\rho_2^2(l)-\frac{1}{4\sqrt{6}}\ ,$$

$$\left[\frac{\Gamma_1(lu)\Gamma_2(l)}{\Omega^2}+\frac{1}{4}\right]\mathrm{Im}\rho_1^2(l)$$
$$=\frac{1}{\sqrt{3}}\cos\phi\rho_0^0(l)-\frac{1}{8\sqrt{6}}\cos\phi\rho_0^2(l)$$
$$+\frac{1}{8}\cos\phi\,\mathrm{Re}\rho_2^2(l)-\frac{1}{4}\cos\phi\ ,$$

$$\left[\frac{\Gamma_1(lu)\Gamma_2(l)}{\Omega^2}+\frac{1}{8}\right]\mathrm{Re}\rho_2^2(l)$$
$$=-\frac{1}{2\sqrt{3}}\rho_0^0(l)+\frac{1}{8}\sin\phi\,\mathrm{Re}\rho_1^1(l)$$
$$-\frac{1}{8\sqrt{6}}\rho_0^2(l)+\frac{1}{8}\cos\phi\,\mathrm{Im}\rho_1^2(l)+\frac{1}{8}\ .$$

For simplicity, the equations are written for a pump laser tuned to a transition between a lower level having $J_l=1$ and an upper level with $J_u=0$. The optical coherences have been eliminated from the equations. Similar equations apply for a transition with an upper level having $J=1$, as was usually the case in our experiments. Which Zeeman coherences are generated for a given pump polarization is clear from these equations. For linear pump polarization ($\phi=0$) the lower-level population is coupled to $\mathrm{Im}\rho_1^2(l)$ and $\mathrm{Re}\rho_2^2(l)$, while for circular pump polarization ($\phi=\pi/2$) the lower-level population is coupled to $\mathrm{Re}\rho_1^1(l)$ and $\mathrm{Re}\rho_2^2(l)$. The solutions of the above equations for high pump laser intensity are

$$\rho_0^0(l)=\tfrac{5}{6},\quad \rho_0^2(l)=\frac{1}{12\sqrt{6}},\quad \mathrm{Re}\rho_1^1(l)=\tfrac{1}{12}\sin\phi\ ,$$
$$\mathrm{Im}\rho_1^2(l)=\tfrac{1}{12}\cos\phi,\quad \mathrm{Re}\rho_2^2(l)=-\tfrac{1}{24}\ .$$

[1] See, for example, J. N. Dodd and G. W. Series, in *Progress in Atomic Spectroscopy Part A*, edited by W. Hanle and H. Kleinpoppen (Plenum, New York, 1978), pp. 639–675.

[2] C. Wieman and T. W. Hansch, Phys. Rev. Lett. **36**, 1170 (1976).

[3] W. Lange and J. Mlynek, Phys. Rev. Lett. **40**, 1373 (1978).

[4] J. Mlynek and W. Lange, Opt. Commun. **30**, 337 (1979).

[5] H. Harde, H. Burggraf, J. Mlynek, and W. Lange, Opt. Lett. **6**, 290 (1981).

[6] S. Burschka and J. Mlynek, Opt. Commun. **66**, 59 (1988).

[7] L. Jozefowski, J. Koperski, and T. Dohnalik, Acta Phys. Pol. A **76**, 895 (1989).

[8] T. Dohnalik, J. Koperski, M. Stankiewicz, J. Zakrzewski, and K. Zyczkowski, Acta Phys. Pol. A **66**, 493 (1984).

[9] R. M. Lowe, D. S. Gough, R. J. McLean, and P. Hannaford, Phys. Rev. A **36**, 5490 (1987); P. Hannaford, R. M. Lowe, and

R. J. McLean, in *Laser Spectroscopy VIII,* edited by W. Persson and S. Svanberg (Springer, Berlin, 1987), pp. 308–309.

[10]R. J. McLean, D. S. Gough, and P. Hannaford, in *Laser Spectroscopy VII,* edited by T. W. Hansch and Y. R. Shen (Springer, Berlin, 1985), p. 220.

[11]Y. H. Zou and N. Bloembergen, Phys. Rev. A **34**, 2968 (1986).

[12]K. H. Drake, W. Lange, and J. Mlynek, Opt. Commun. **66**, 315 (1988).

[13]P. E. G. Baird, M. Irie, and T. D. Wolfenden, J. Phys. B **22**, 1733 (1989).

[14]L. M. Barkov, D. A. Melik-Pashayev, and M. S. Zolotorev, Opt. Commun. **70**, 467 (1989).

[15]F. Schuller, M. J. D. Macpherson, and D. N. Stacey, Opt. Commun. **71**, 61 (1989).

[16]C. Parigger, P. Hannaford, W. J. Sandle, and R. J. Ballagh, Phys. Rev. A **31**, 4043 (1985); C. Parigger, P. Hannaford, and W. J. Sandle, *ibid.* **34**, 2058 (1986).

[17]A. P. Ghosh, C. D. Nabors, M. A. Attili, J. E. Thomas, and M. S. Feld, Phys. Rev. Lett. **53**, 1333 (1984).

[18]R. E. Teets, F. V. Kowalski, W. T. Hill, N. Carlson, and T. W. Hansch, Proc. Soc. Photo-Opt. Instrum. Eng. **113**, 80 (1977).

[19]M. Ducloy, Phys. Rev. A **8**, 1844 (1973).

[20]P. Hannaford, Contemp. Phys. **24**, 251 (1983).

[21]B. J. Dalton, D. S. Gough, P. Hannaford, and R. M. Lowe, J. Phys. B **15**, L515 (1982); B. J. Dalton, C. R. Allton, P. Hannaford, R. M. Lowe, and D. S. Gough, *ibid.* **20**, 267 (1987).

[22]Chr. Tamm, E. Buhr, and J. Mlynek, Phys. Rev. A **34**, 1977 (1986).

[23]E. Buhr and J. Mlynek, Phys. Rev. A **36**, 2684 (1987).

[24]R. B. Partridge and G. W. Series, Proc. Phys. Soc. **88**, 983 (1966).

[25]M. Elbel, B. Niewitecka, and L. Krause, Can. J. Phys. **48**, 2996 (1970); B. Niewitecka and L. Krause, *ibid.* **51**, 425 (1973); **51**, 993 (1973).

[26]W. E. Baylis, in *Progress in Atomic Spectroscopy Part B,* edited by W. Hanle and H. Kleinpoppen (Plenum, New York, 1979), pp. 1227–1297.

[27]E. Lewis, Phys. Rep. **58**, 1 (1980).

[28]W. Happer, Rev. Mod. Phys. **44**, 169 (1972).

[29]J. P. Barrat, D. Casalta, J. L. Cojan, and J. Hamel, J. Phys. (Paris) **27**, 608 (1966).

[30]J. P. Faroux and J. Brossel, C. R. Acad. Sci. Ser. B **261**, 3092 (1965); **263**, 612 (1966); **264**, 1452 (1967).

[31]R. Pepperl, Z. Naturforsch. **25A**, 927 (1970).

[32]B. Laniepce and J. P. Barrat, C. R. Acad. Sci. Ser. B **264**, 146 (1967).

[33]W. J. Tomlinson and R. L. Fork, Phys. Rev. Lett. **20**, 647 (1968).

[34]P. R. Berman and W. E. Lamb, Phys. Rev. **187**, 221 (1969).

[35]A. Omont, J. Phys. (Paris) **26**, 26 (1965).

[36]E. L. Lewis and L. F. McNamara, Phys. Rev. A **5**, 2643 (1972).

[37]A. Omont, Prog. Quantum Electron. **5**, 69 (1977).

[38]W. Happer, Phys. Rev. B **1**, 2203 (1970).

[39]C. H. Wang and W. J. Tomlinson, Phys. Rev. **181**, 115 (1969).

[40]C. Cohen-Tannoudji, J. Phys. Radium **24**, 653 (1963).

[41]M. Leduc and J. Brossel, C. R. Acad. Sci. Ser. B **266**, 287 (1968).

[42]J. Marek and P. Munster, Astron. Astrophys. **62**, 245 (1978).

[43]W. E. Baylis, in *Progress in Atomic Spectroscopy Part A,* edited by W. Hanle and H. Kleinpoppen (Plenum, New York, 1979), pp. 207–261; and private communcation.

[44]V. D. Venedin, V. N. Kulyasov, A. L. Kurbatov, N. V. Rodin, and M. V. Shubin, Opt. Spektrosk. **62**, 737 (1987) [Opt. Spectrosc. (USSR) **62**, 439 (1987)].

[45]L. M. Barkov, M. S. Zolotarev, and D. A. Melik-Pashaev, Opt. Spektrosk. **66**, 495 (1989) [Opt. Spectrosc. (USSR) **66**, 288 (1989)].

[46]E. B. Aleksandrov, V. N. Kotylev, K. P. Vasilevskii, and V. N. Kulyasov, Opt. Spektrosk. **54**, 3 (1983) [Opt. Spectrosc. (USSR) **54**, 1 (1983)].